Bacterial Synthesis of PHA Block Copolymers

Erik N. Pederson, Christopher W. J. McChalicher, and Friedrich Srienc*

Department of Chemical Engineering and Materials Science and the BioTechnology Institute, University of Minnesota, Minneapolis/St. Paul, Minnesota 55455/55108

Received December 30, 2005; Revised Manuscript Received March 28, 2006

Polyhydroxyalkanoates (PHA) containing block copolymers were synthesized in *Cupriavidus necator* using periodic substrate addition. Poly(3-hydroxybutyrate) (PHB) segments were formed during fructose utilization. Pulse feeds of pentanoic acid resulted in the synthesis of 3-hydroxyvalerate monomers, forming poly(3-hydroxybutyrate-*co*-3-hydroxyvalerate) (PHBV) random copolymer. PHA synthesis was controlled using analysis of oxygen uptake and carbon evolution rates from the bioreactor off-gas. A combination of characterization techniques applied to the polymer batches strongly suggests the presence of block copolymers: (i) Thermodynamically stable polymer samples obtained by fractionation and analyzed by differential scanning calorimetry (DSC) and nuclear magnetic resonance spectroscopy (NMR) indicate that some fractions, representing approximately 30% of the total polymer sample, exhibit melting characteristics and nearest-neighbor statistics indicative of block copolymers, (ii) preliminary rheology experiments indicate additional mesophase transitions only found in block copolymer materials, (iii) dynamic mechanical analysis shows extension of the rubbery plateaus in block copolymer samples, and (iv) uniaxial extension tests result in differences in mechanical properties (modulus and elongation at failure) expected of similarly prepared block copolymer and single polymer type materials.

Introduction

There is substantial interest for sustainable technologies based on biorenewable resources to supplement or replace the existing need of nonrenewable resources. Exploration into alternative plastics derived from biologically renewable resources over the past 20 years has resulted in a few commercially viable polymers that may compete with some traditional petrochemical polymers.[1−3] Polyhydroxyalkanoates (PHAs) represent one class of biopolymers. PHAs are synthesized by various microorganisms as a carbon and energy storage compound during unbalanced growth.[4] PHAs gained initial interest as a green alternative to petrochemical-derived polymers, because they are biodegradable, biocompatible, and synthesized from biorenewable resources. Over 150 possible monomer units offer a broad range of polymer properties that can compete with petrochemically derived plastics such as polypropylene and polyethylene.[5]

In addition to monomer variability, polymer microstructure is another method of developing new and favorable properties. For example, block copolymers consist of polymer chains containing two or more unique polymer regions covalently bonded together.[6] This structure captures the properties of each block and potentially achieves new properties not available by polymer blending. Possible block copolymer structures include A−B diblock, A−B−A or A−B−C triblock, or $(AB)_n$ repeating multiblocks, among others. A review of block copolymers and possible morphologies is detailed in Bates et al.[7] Reports of PHA block copolymer synthesis indicate that traditional chemical synthesis techniques have been successful in generating block copolymers using PHAs. Examples of PHA-related block copolymers include poly(3-hydroxybutyrate) blocks balanced with blocks of poly(6-hydroxyhexanoate),[8] poly(3-hydroxyoctanoate),[9] monomethoxy-terminated poly(ethylene glycol) (mPEG),[10] and poly(ethylene glycol).[11,12]

* Corresponding author. Dr. Friedrich Srienc, 240 Gortner Lab, 1479 Gortner Ave., St. Paul, MN 55108, 612-624-9776; Srienc@umn.edu.

The gram-negative bacterium *Cupriavidus necator* (formerly *Wautersia eutropha*, *Ralstonia eutropha*[13,14]) is capable of storing high quantities of so-called "short chain length" PHA, that is, PHA composed of monomers with three to five carbons, during nutrient limiting conditions. The kinetics and dynamics of PHA synthesis in *C. necator* have been described with computer models[15,16] and detailed mathematical models.[17] Previously, synthesis of poly(3-*R*-hydroxybutyrate)-*block*-poly(3-*R*-hydroxybutyrate-*co*-3-*R*-hydroxyvalerate) (PHB-*b*-PHBV) was demonstrated by alternating the substrates responsible for PHA synthesis.[17] During this polymerization, 3-*R*-hydroxybutyrate monomer (3HB) was continually produced via fructose catabolism. The additional feeding of valerate resulted in the generation of 3-*R*-hydroxyvalerate monomer (3HV) in addition to 3HB, leading to synthesis of the PHBV block. The feeding of valerate was based on a model that predicted the block copolymer compositional distribution as a function of the valerate cofeeding time.[18] The valerate and fructose cofeeding time is the length of time valerate is present in the bioreactor and is available for PHBV production. This cofeeding window is complemented by a suitable fructose-only availability that is responsible for synthesis of PHB homopolymer. The two regimes combine to form a single cycle in the polymer production scheme. This synthesis considers fructose-only feeding times that synthesizes equal portions of each block when combined with the respective cofeeding time.

Previous attempts at the implementation of this system utilized a time-based feeding program that failed to adjust for changing cell physiology that results in slowing of the polymerization kinetics.[18,19] This phenomenon would require variation in the quantity of valerate added to the reactor to maintain the appropriate cofeeding time. To account for these variations and make shorter time switches possible, an online mass spectrometry (MS) feedback control system is implemented here. This system monitors the valerate consumption kinetics and controls the valerate feeding based on the value of the respiratory

10.1021/bm0510101 CCC: $33.50
Published on Web 05/04/2006

quotient (RQ), a dimensionless ratio of the rates of carbon evolution and oxygen uptake. This system was previously used for synthesis of PHA core−shell granules within *C. necator*, and a detailed explanation of the MS physiological response during growth and PHA synthesis was presented.[20]

In this paper, we discuss the implementation of online MS feedback control for PHB-*b*-PHBV synthesis, as well as comparisons of some limited characteristics of the resulting polymer materials. This synthesis method is an improvement, because adjustments to changing cellular dynamics are automatic. Further, this instrumentation allows easy variation of the cofeeding window. Block copolymer systems were synthesized with cofeeding times varying from 8 to 32 min. Polymer films were made to investigate the novel mechanical properties achieved by the new block copolymer systems and compared to existing random copolymer samples. The differences seen in this comparison provide strong support of the assertion that block copolymer structures have been incorporated into the bacterially synthesized polymer material.

Material and Methods

a. Cell Cultivation. Polymer was made in a two-step process involving growth on complex medium, harvesting of cells using a continuous centrifuge (Sharples model T-1P, AMF Beaird Inc., Shreveport, LA), and transfer of cells to the minimal medium for polymer production. Polymer-rich biomass was harvested using the same continuous centrifuge system. The complex medium used for cell growth is described elsewhere[21] with the substitution of 5 g/L Primotone RL (Quest Int., Hoffman Estates, IL) for beef extract. The minimal medium used for polymer accumulation is described elsewhere.[20] During polymer production, the minimal medium initially contained 0.2 g/L $(NH_4)_2SO_4$ to allow adaptation from complex to minimal medium containing valeric acid.[22] Frozen master culture of *C. necator* H-16 (frozen in 40% v/v glycerol) was used to prepared the bioreactor innoculum. Valeric acid was brought to a final concentration of 100 g/L and pH 7 (distilled water and 6 M NaOH) and was fed into the reactors by a peristaltic substrate pump (Watson-Marlow, Wilmington, MA). Fructose was present at an initial concentration of 20 g/L and remained in excess during polymer synthesis. The 10 L bioreactors (B. Braun Biotech, Allentown, PA) were operated at 800 rpm, pH 7 (6 M NaOH and 30% H_3PO_4), and 1 vvm air flow. Dissolved oxygen concentration remained above 40% during growth and polymer accumulation under the given stirring and aeration conditions. All chemical and media components were purchased from Sigma (St. Louis, MO) except fructose (ICN Biomedicals, Aurora, OH) and ammonium sulfate (Mallinckrodt, Hazelwood, MO).

b. Monitoring with Mass Spectometry. A Prima δB mass spectrometer (ThermoOnix, Houston, TX) was interfaced with the bioreactors for exhaust gas monitoring utilizing a 32-valve sampling port as described previously.[20] Calculation of the carbon dioxide evolution rate (CER) and oxygen uptake rate (OUR) became possible through analysis of the compositions in the inlet and exhaust streams. The CER and OUR are global mass balances on CO_2 and O_2, respectively, and have dimensions of millimoles per liter per hour (mmol L^{-1} h^{-1}).[23] The respiratory quotient (RQ) is the CER/OUR ratio and is dimensionless. Calculation of these values was performed by the MS Gasworks software (ThermoOnix, Houston, TX).

c. Feedback Control System. Dynamic data exchange (DDE) was implemented to share online data in real time between the MS Gasworks software and the MFCS bioreactor software (B. Braun Biotech, Allentown, PA). A Microsoft Excel spreadsheet was used to permit data exchange without direct software communication. The OUR, CER, and RQ were fed from the gasworks software into the MFCS software, allowing algorithms to control the substrate pump during copolymer production.[20] An example substrate pump control flow sheet (Boolean logic) for valerate cofeeding is depicted in Figure 1.

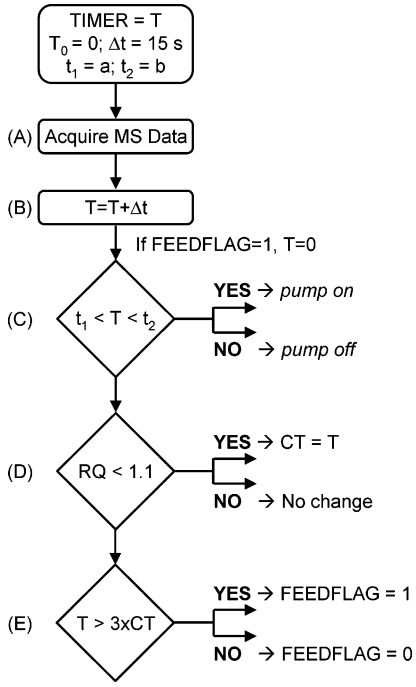

Figure 1. The diagram illustrates the feedback control responsible for block copolymer synthesis. This system monitors and controls valerate pulse additions into the bioreactor. After input of the desired setpoints, MS data is acquired by the control software (A). A new sample from the MS triggers incrementation of the TIMER variable (B). If the FEEDFLAG trigger equals zero, TIMER is reset. TIMER is compared to the feed window to determine polymerization regime (C). The presence of valerate is monitored by the value of RQ and determines valerate CONSUME-TIME (CT) (D). Finally, TIMER is compared to CT to determine the restart of the substrate switch.

d. Bioreactor Analytics. Cell dry weight (CDW) analysis was performed gravimetrically. CDW samples were then used for polymer analysis. PHA content and composition was determined by propanolysis and gas chromatography as described elsewhere.[24]

e. Polymer Isolation. Recovered polymer-rich biomass was frozen in liquid nitrogen and lyophilized in a Virtis (Gardiner, New York) freeze-dryer overnight. Polymer from approximately 5−10 g of freeze-dried biomass was extracted using 100 mL of boiling chloroform and a Soxhlet apparatus for 2 days. The extracted polymer was precipitated with 5 volumes of methanol, filtered, and dried in a fume hood.

f. Film Casting. Films were cast by dissolving approximately 400 mg of unfractionated polymer in either 10 mL of chloroform at 60 °C or 1,2,4-trichlorobenzene (TCB) at 140 °C. The TCB solutions were cast in an oven at 130 °C, and the chloroform solutions were cast at room temperature in flat-bottom Petri dishes under proper ventilation.

g. Parallel Plate Rheology. Rheology was conducted using an ARES series rheometer with 7.9 mm parallel plate geometry and a gap thickness of approximately 1 mm. Test conditions included a 5 °C/min ramp, a 1 Hz oscillatory strain, 8% strain control to limit sample deformation, and compensation for thermal expansion of the apparatus to keep the real gap between plates constant. Samples were loaded at 170 °C and immediately subjected to the test conditions. The test measured the storage modulus (G'), loss modulus (G''), and tan δ as a function of temperature. The samples were analyzed during cooling from 170 to 80 °C. The temperature was then ramped back to 175 °C under the same test conditions to acquire the response during heating. Four samples from each polymer system were loaded for testing and were subjected to two consecutive temperature cycles. Data presented is from a representative sample portraying trends and averages indicative of the population. The discontinuity of the data at the lower temperature is due to the time delay caused by the manual turnaround of the testing

program. The observed differences represent the transient motion toward the equilibrium state during this resting period.

h. Dynamic Mechanical Analysis. A Perkin-Elmer 7e dynamic mechanical analyzer was used to investigate the complex storage (E') and loss moduli (E'') as a function of temperature. Samples were cut into rectangular strips approximately 3 mm wide, 10 mm long, and 0.10 mm thick. Samples were scanned from −30 to 180 °C at 5 °C/min and a frequency of 1 Hz. Amplitude control was implemented to control sample strain to <1%. Temperature to flow (T_{flow}) was recorded as the temperature where the film failed. Samples were tested five times for each polymer system.

i. Tensile Testing. Tensile testing was performed at room temperature on samples prepared from solvent-cast films. Films were annealed at 135 °C for 45 min 1 day prior to testing. The dimensions of test samples were 1 mm wide by 0.1 mm thick by 10 mm long. The initial gap between clamps was approximately 5 mm. Films were stretched on a MicroBionix uniaxial extender with a 5 N load cell (MTS Systems Corporation) at a pull rate of 5 mm/min until failure (approximate strain rate of 1 min^{-1}). TestStar II V4.0 (MTS Systems Corporation) software was used to control the instrument and to collect data. Two films were cast for each polymer system, and five samples were excised and tested from each film. Reported curves are individual tests representative of the population in important markers such as extension until failure, modulus, and tensile strength.

j. Fractionation of Polymers. Polymer samples were dissolved in warm chloroform at 5 g/L and allowed to stir overnight to cool to room temperature. Heptane was added until a precipitate formed.[25] Precipitated samples were centrifuged for 10 min at 4000 g to sediment the polymer. Heptane addition and subsequent centrifugation continued until all polymer was recovered.

k. Differential Scanning Calorimetry. Differential scanning calorimetry (DSC) was performed on a TA Instruments-Waters LLC Q1000 (New Castle, DE) using 5 mg of fractionated polymer samples. Samples were heated to a final temperature of 180 °C at a 10 °C/min ramp to observe the melting points (T_m) of the crystalline sample. The samples were held at 180 °C for 1 min and then quenched rapidly to −40 °C. The samples were reheated at 10 °C /min to 180 °C to observe the glass transition (T_g) and T_m. The temperatures reported are peak values.

l. Nuclear Magnetic Resonance. Samples of fractionated polymer were dissolved in deuterated chloroform at 100 mg/mL. ^1H signals were used to determine the polymer composition of HV and HB units, and ^{13}C signals were used to detail the monomer sequence.[26]

m. Molecular Weight Analysis. Select samples were analyzed for molecular weight distribution by high-temperature gel permeation chromatography. A Polymer Labs PL GPC 220 high-temperature chromatograph (Amherst, MA) was operated with 3 PL-gel 10 μm mixed B columns in series at 140 °C with 1,2,4-triclorobenzene (TCB) as the mobile phase. Polystyrene standards (PS) were used to create the calibration curve. Molecular weights are reported as PS equivalent values.

Results

Experimental Design. Synthesizing block copolymers within any polymerization scheme requires control of monomer availability. As stated earlier, *C. necator* synthesizes PHB from fructose during stationary phase induced by nitrogen limitation. The additional feeding of valerate results in synthesis of PHBV, a random copolymer containing 3-*R*-hydroxyvalerate (3HV) and 3-*R*-hydroxybutyrate (3HB) units. The periodic feeding of valerate was controlled to synthesize block copolymer containing PHB and PHBV blocks. Restricting the cofeeding of valerate to specific periods of time within a cycle was realized by assessment of cell physiology via data collected by the online MS system.

Table 1. Predicted Components of Biologically Synthesized Block Copolymers[a]

block sample	switching time (min)	composition di	composition tri
block-8	8	21%	22%
block-10	10	26%	23%
block-14	14	36%	24%
block-32	32	48%	10%

[a] The block copolymer samples are labeled according to their valerate cofeeding time. The predicted block copolymer composition is reported.

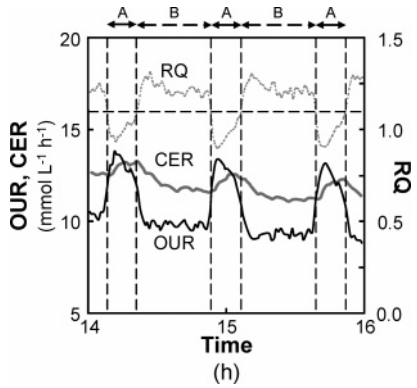

Figure 2. Detailed view of periodic polymer synthesis. Three trends are represented; OUR, CER, and RQ; over a 2 h period. The periods marked A represent PHBV synthesis where both fructose and valerate are present in the bioreactor. The B periods represent PHB synthesis, when only fructose is available as a substrate. The horizontal dashed line indicates the RQ value used to distinguish between the two polymerization regimes. Vertical dashed lines indicate boundaries for the feeding windows.

To optimize block copolymer synthesis, a previously reported mathematical model was considered.[18,19] Model predictions indicate that cycles consisting of 30 min valerate and fructose cofeeding (PHBV synthesis) followed by 60 min of PHB synthesis on only fructose optimizes the ratio of 50:50 diblocks within the biological polymerization. Further, the fraction of triblock copolymer with equal composition of PHB and PHBV is optimized using a valerate and fructose cofeeding time of 12.5 min and the corresponding fructose feeding time of 25 min.[18,19]

The experimental conditions for different block copolymer synthesis experiments and predicted block copolymer compositions from the previously discussed model[18,19] are summarized in Table 1 (note: the number in the experiment identification number refers to the valerate and fructose cofeeding time in minutes). Valerate consumption increased oxygen demand, leading to a larger OUR and a decreased RQ. This physiological response served as the indicator in the control scheme for valerate presence in the bioreactor. The cofeeding time was controlled to a precision of 15 s because of the limitations of the MS sampling cycle. This corresponds to a maximum error of approximately 3% for the shortest cofeeding time considered. Figure 2 shows three consecutive pulses with dotted lines indicating the boundaries for the different feed windows. This figure illustrates the precision, tightness, and periodicity of the synthesis regimes.

The block copolymer synthesis approach is complicated by the fact that the synthesis does not occur synchronously on all polymer chains such as during true living polymerization. This happens because of random chain initiation and termination events. This makes analytical techniques to characterize block copolymers and to demonstrate their presence more complicated.

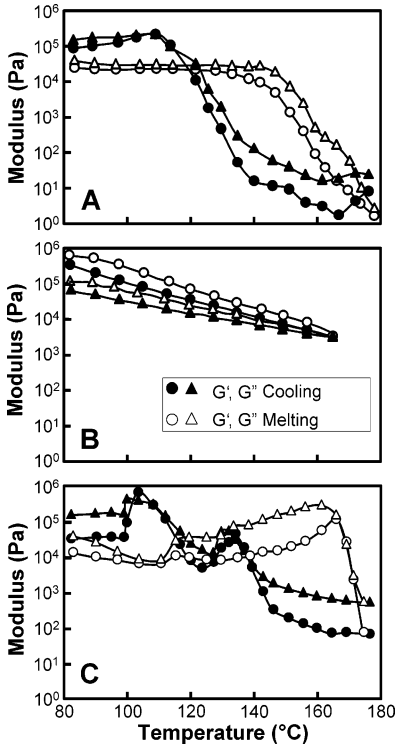

Figure 3. Parallel plate rheological data from polymers extracted from biomass. Temperature sweep tests for homogeneous PHB (A), 29% HV copolymer (B), and **block-10** (C).

The synthesized material consists of a mixture of different block copolymers of different molecular weights and a distribution of individual blocks within a chain. We have previously described these expected distributions estimated with theoretical models.[17,18]

To show experimentally that the bacterial system is able to synthesize block copolymers, we resorted to physical characterization techniques that provide indirect evidence for the existence of block copolymers. The presence of block copolymer results in distinct properties of the obtained material that are different from the properties of similarly prepared pure homopolymers or of random copolymers.

Mechanical Characterization. Isolated polymers were characterized by parallel plate rheology to examine the melt behavior. Figure 3 shows the response profiles of the storage and loss moduli (G' and G'') versus temperature for three biologically prepared samples: PHB homopolymer, 29% HV random copolymer, and **block-10**, a 22% HV block copolymer synthesized using a 10 min cofeeding window per cycle. As the PHB homopolymer cooled, crystallization initiated at 155 °C, and the storage modulus reached a plateau at 122 °C (Figure 3A). A hysteresis loop was observed for the PHB homopolymer upon reheating, and an extended modulus plateau was observed until 147 °C when a dropoff was observed associated with the melting transition. The 29% HV random copolymer showed different behavior than the PHB homopolymer. For the random copolymer sample (Figure 3B), the storage and loss moduli increased linearly as the temperature decreased. Upon heating, hysteresis behavior was observed. The modulus plateau extended to 90 °C when the moduli decreased and mirrored the cooling trend.

Figure 3C shows the rheological data for **block-10** block copolymer sample. The data were compared to the PHB and 29% HV copolymer to observe any differences resulting from synthesis of block copolymer. Similar to PHB, crystallization initiated during cooling at 155 °C and ceased at 130 °C. At temperatures below 130 °C, the moduli exhibited two peaks before a plateau was reached at 100 °C. These secondary transitions are reproducible and have not been seen in any PHB or PHBV random copolymer sample. While this behavior is under further investigation, the rearrangement of block copolymer microstructures are the likely cause of these responses. Upon heating, the moduli initially decreased at a rate similar to the 29% HV random copolymer. However, at 110 °C the moduli began to increase until the melt transition at 167 °C. This trend was not expected and was only observed in block copolymer samples.

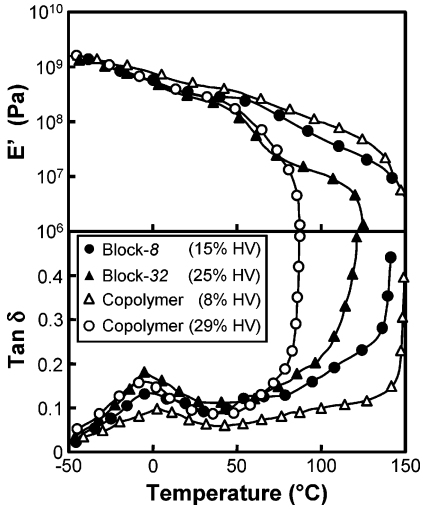

Figure 4. DMA of polymer films cast from chloroform. The E' (6a) and tan δ (6b) for block copolymers and random copolymer films are shown. The polymers are labeled in the legend and include the overall HV% in the film.

Dynamic mechanical analysis (DMA) was also used to investigate the dynamic storage modulus (E'), loss modulus (E''), and tan δ of the solvent cast films. In PHBV random copolymers, the melting temperature (T_m), glass transition temperature (T_g), temperature to flow (T_{flow}), and moduli decrease as HV% increases.[27] Figure 4 shows the E' and tan δ traces for two block copolymer samples and two random copolymers cast from chloroform. The DMA curves of block copolymer samples were compared to random PHBV copolymers and PHB−PHBV blends with the same fraction of incorporated HV to determine if the films had novel material properties. **Block-8** containing 15% HV had properties similar to the 8% copolymer. Even though **block-8** contained twice the overall HV% content and a slightly lower modulus, its T_{flow} was extended to equal that of the 8% HV copolymer. This same trend was observed in **block-32** containing 25% HV when compared to the 29% random copolymer. With only slightly less HV content, the block copolymer T_{flow} was 125 °C, 37 °C higher than the similar HV% copolymer. The two moduli curves were similar until 77 °C when the block copolymer modulus experienced a secondary plateau that increased the T_{flow}.

Block copolymer films were also cast from 1,2,4-trichlorobenzene (TCB) because chloroform could not completely dissolve all synthesized polymer. TCB successfully dissolved all samples when heated to 140 °C. Figure 5 shows the E' and tan δ for the same four polymer films cast from TCB as shown in Figure 4. **Block-8** again had a storage modulus that mirrored the 8% HV random copolymer at a slightly lower value but now had a T_{flow} of 164 °C compared to only 151 °C for the random copolymer. **Block-32** (25% HV) had a similar storage modulus to **block-8** and a T_{flow} of 161 °C, which was

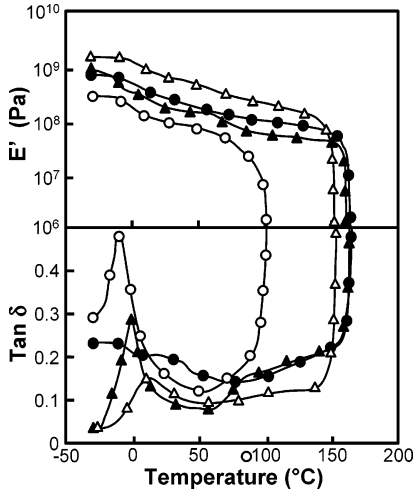

Figure 5. DMA of TCB cast block copolymer films. The *E*′ (7a) and tan δ (7b) for block copolymers and copolymers cast from TCB are shown. Shown are random copolymer samples containing 29% HV (○) and 8% HV (●) and **block-8** (▲) and **block-32** (△).

Table 2. Properties of Block Copolymer and Random Copolymer Bulk Samples[a]

		chloroform		TCB			
	HV	T_g	T_m	T_g	T_m	M_n	
sample	%	°C	°C	°C	°C	10^3	PDI
block-8	15	−8, 7	142	−9, 8	164	99.4	2.02
block-14	13			−4, 9	161	100.2	2.09
block-32	23	−5, 6	125	−1	161	106.8	2.07
random copolymer	29	−10	87	−10	101	99.3	2.02
random copolymer	8	10	151	17	151	107.5	2.04

[a] Percent 3HV repeat unit is reported. Films were cast from either TCB or chloroform and tested by DMA. The T_g and T_m are reported. Molecular weight and polydispersity were determined by GPC and are also reported.

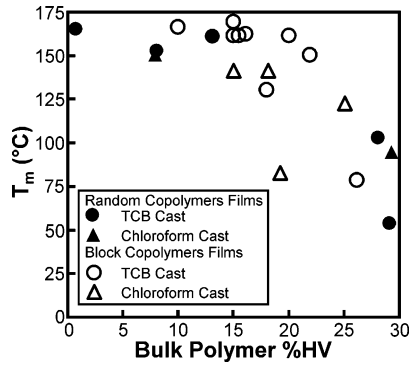

Figure 6. Flow temperature vs degree of 3HV incorporation. The T_{flow} (T_m) is plotted for block copolymer and random copolymer films cast from TCB and $CHCl_3$. The samples are plotted accordingly to the HV%, casting solvent, and block copolymer vs random copolymer. The T_{flow} was determined with DMA.

significantly higher than the 101 °C T_{flow} for the 29% HV random copolymer. Again, the increased T_{flow} was due to a secondary modulus plateau that occurred near the T_{flow} of the random copolymer. This secondary plateau in the storage modulus was common for block copolymer samples but was not seen for random copolymers or blends. A summary of the T_{flow} and T_g determined by the tan δ peak are shown in Table 2 for block copolymer and random copolymer samples. Figure 6 shows the T_m as a function of HV% in the samples. The films cast from chloroform had lower T_{flow} values than the TCB cast films. Also, the block copolymer samples had equal or larger

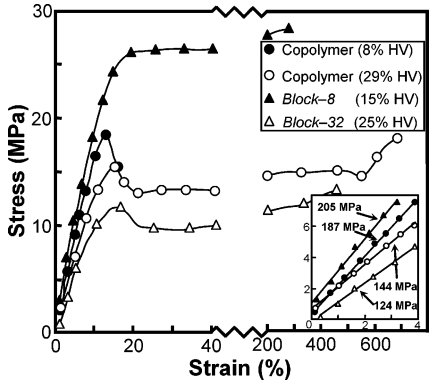

Figure 7. Stress−strain curves from tensile testing. The stress−strain curves from tensile testing are shown for the random copolymer samples containing 29% HV (○) and 8% HV (●) and **block-8** (▲) and **block-32** (△). The insert shows the low strain used to calculate the Young's modulus.

T_m values than random copolymers of the same HV content. Between the two sets of DMA data, the clear extension of the rubbery plateau is likely to be a direct effect of block copolymer incorporation.

The tensile properties of the TCB solvent-cast films were determined to compare the material properties of random copolymer versus block copolymer films. Four samples were tested: 8% HV random copolymer, 29% HV random copolymer, **block-32** (25% HV), and **block-8** (15% HV). Figure 7 shows representative stress−strain curves for the four samples. The 8% HV random copolymer exhibits characteristics of a brittle, highly crystalline polymer. The strain at failure was less than 15% and showed no little necking or plastic deformation. The material had a Young's modulus of 187 MPa and an ultimate tensile strength of 19 MPa. The general properties of the 29% HV random copolymer were indicative of an amorphous thermoplastic. Plastic deformation began at 11%, and the sample continued to draw until fracture occurred at 900% strain. The film had a Young's modulus of 144 MPa, lower than the 8% HV random copolymer sample. The ultimate tensile strength was 15 MPa.

Block-8 containing 15% HV showed results between the two random copolymer samples with respect to the strain at failure and the plastic deformation. Much like the 29% HV copolymer, plastic deformation began at 11%. The Young's modulus (205 MPa) and ultimate tensile strength (26 MPa) were comparable to those of the 8% HV random copolymer sample. However, the strain to failure was 250%, less than the valerate-rich random copolymer sample but greater than the comparable 8% HV sample. **Block-32** had the lowest modulus (124 MPa) and ultimate tensile strength (12 MPa) but maintained a large strain at failure of 575%.

Physical and Thermal Characterization. These same polymers were analyzed for molecular weight distribution using gel permeation chromatography (GPC). These results are outlined in Table 2. While it is difficult to control the degree of polymerization and polydispersity within a biological polymerization scheme, it appears that all four samples have similar M_n and polydispersity index (PDI) values. These values are generally around 10^5 and 2 for M_n and PDI, respectively.

A combination of tests was employed to calculate the block copolymer yield by determining the physicochemical properties of the polymers. The first characterization step attempted to isolate the block copolymer from the bulk PHB homopolymer and PHBV random copolymer. PHA copolymers are biologically synthesized with a broad chemical compositional distribution

Table 3. Characterization of the Fractions of **Block-14** Obtained from Solvent/Nonsolvent Fractionation[a]

fraction	heptane %	3HV %	quantity % of stock	T_g °C	T_m °C	D stat
F1	47	0	46	6	143, 166	ND
F2	55	9	23	5	140, 166	1.9
F3	58	22	20	−1, 5	79, 140, 159	9.1
F4	62	44	8	−8, −4	80, 140, 160	3.1

[a] The reported T_g and T_m were determined by DSC. Other reported values for each fraction are as follows: percentage of total heptane used to effect precipitation, percent 3HV repeat unit, quantity of fraction with respect to stock sample, and the NMR *D* statistic.

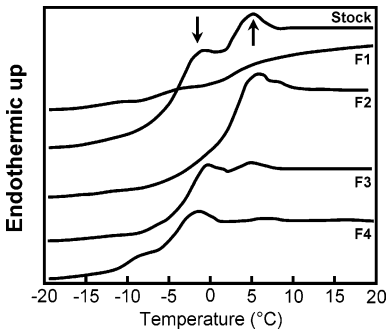

Figure 8. DSC trace of T_g for fractionation of **block-14**. The fractions are the fractions as depicted in Table 3. The two arrows represent the T_g for PHBV (−3 °C) and PHB (5 °C). The fractions contain one or both of these transitions.

(CCD).[27] Yoshie et al. reported a fractionation technique to separate PHA copolymer into fractions that contained narrow property distributions. This technique has also been shown to separate physical blends of PHB and PHBV into fractions of similar composition.[19] Because block copolymers of PHB and PHBV cannot physically separate, fractions containing block copolymers would exhibit properties of both polymers.

The fractionation results of block copolymer experiment **block-14** are detailed in Table 3. The first fraction (F1) contained 46% of the initial quantity of polymer with no recovery of units containing 3HV within the monomer sequence. Another 23% of total polymer was recovered in the second fraction (F2), containing 55% 3HV. The quantity polymer in the final two fractions (F3 and F4) represent 20% and 8% of the total polymer and had 22% and 44% 3HV, respectively. Three percent of initial polymer was not recovered.

The fractions were characterized to determine their thermochemical properties with differential scanning calorimetry (DSC). Important temperatures as determined from DSC are also detailed in Table 3. The DSC traces for fractionation of **block-14** are shown in Figures 8 and 9. Two T_m's were expected due to recrystallization during heating.[28] Fractions 1 and 2 (F1, F2) contain two T_m and one T_g values, characteristic of low HV% copolymer. F3 and F4 display three T_m and two T_g values, implying both PHB and PHBV phases were present. Because the fractionation would have separated a simple blend of the two phases, the traces suggest that F3 and F4 are predominately block copolymer.

The fractions were examined with ^{13}C NMR to determine the monomer sequence distribution. Analysis of the diad peaks revealed the nearest monomer neighbor distribution in the fraction and the *D* statistic of $(F_{VV}F_{BB})/(F_{BV}F_{VB})$ was determined where F_{BB} represents the fraction of HB units neighboring a HB unit, and so forth.[26] Statistically random copolymers would have a *D* value near 1, while *D* values greater than 1.5 imply the polymer contains either blocky regions or a blend of

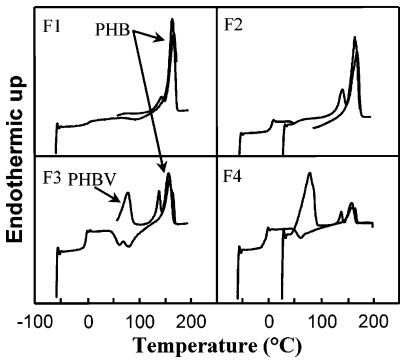

Figure 9. DSC T_m data for fractionation of **block-14**. The fractions are the fractions as depicted in Table 3. The T_m's are observed prior to annealing. The PHB and PHBV peaks are labeled in F1 and F3 and correspond to approximately 160 °C and 80 °C, respectively.

polymers.[25] Analysis of our fractions yielded F3 with the largest *D* value of 9.1 compared to only 3.1 for F4 and 1.9 for F2.

Discussion

Integration of an off-gas MS allowed precise control of valerate additions to the bioreactor for synthesis of PHA block copolymers in *C. necator*. The physiological difference between PHB and PHBV synthesis was linked to the RQ value, which was ultimately used as the control trigger. Cofeeding windows were varied from 8 min to 32 min per period to synthesize different block copolymer systems.

Polymer systems were synthesized in bacteria, isolated, and used to make solvent-cast films to compare the film properties of block copolymers to those of random copolymers and blends. Block copolymer samples exhibited secondary transitions in the storage modulus that were not displayed in random copolymers. These secondary transitions could result from changes in polymer microstructure or morphology due to the presence of block copolymer and the stresses resulting from the oscillatory strain and temperature ramp. Adding to the intrigue is the unique behavior found in the storage modulus during DMA testing. The block polymer films experienced an increased temperature to flow compared to simple copolymers and blends containing the same percentage of 3HV repeat unit. This occurred due to elongation of the rubbery plateau, a phenomenon commonly associated with block copolymers. To further support block copolymer incorporation as the cause of the extended rubbery plateau, molecular weight analysis was completed. It was found that the molecular weights of the samples were well within the range of each other. In addition, the variability of the molecular weights does not match the expected dependence of the length of the rubbery plateau. Therefore, it can be concluded that the dominant effect is not differences in molecular weight, but rather is likely caused by the polymer microstructure.

The material properties of the block copolymer films were examined to determine the tensile properties. **Block-8** was an interesting sample having the largest ultimate tensile strength and Young's modulus, while still being ductile and having a strain at failure of 250%. This sample combined strength and elastomeric behavior, a desirable characteristic of thermoplastic elastomers. This is likely the result of incorporating block copolymer microstructure in the films. The **block-32** sample also had a large strain at failure but did not have a larger modulus or ultimate tensile strength than the similar HV composition random copolymer.

It is interesting to note that all the films tested had lower Young's moduli and ultimate tensile strengths than expected

from other literature sources stated earlier. One likely explanation is the sample preparation and annealing methods reported here. Samples were tested 1 day after annealing and likely had not achieved equilibrium crystallinity. The crystallization rate would be expected to differ between random copolymer samples and those that contain block copolymer due to different size polymer domains. Repression of crystallinity would lower the moduli and ultimate tensile strengths and could increase the strain at failure. Further studies are underway comparing the tensile properties as a function of time and with respect to annealing and degree of crystallinity.

Another observed trend was the high T_{flow} for films cast from TCB when compared to the chloroform-cast films. A likely explanation is the complete dissolution off all crystalline PHB regions when the solvent was heated to 140 °C. The chloroform was unsuccessful in dissolving all samples and likely excluded some PHB domains from the film matrix resulting in the overall lower T_{flow} values. This trend is shown in Figure 6.

The solvent/nonsolvent fractionation experiment and subsequent DSC and NMR analysis provided further evidence that block copolymers were indeed synthesized biologically. Four fractions were recovered, each containing different degrees of 3HV incorporation (Table 3). Because it contained no 3HV, the first fraction is obviously homogeneous PHB synthesized during the fructose-only polymerization scheme as well as residual PHB stemming from growth-associated production of PHB in *C. necator*. The DSC trace supports this finding, as only a singular T_g was observed. Because there was no 3HV in the system, the *D* statistic could not be determined because the ratio is undefined. It is highly likely that the second fraction is a quantity of PHBV random copolymer with low levels of 3HV incorporation. As stated earlier, these materials tend toward a singular glass transition as well.

The third and fourth fractions indicate compositions, glass transitions, and *D* statistics that are commensurate with A−B or A−B−A block copolymers and fractions of PHBV random copolymers. Diblocks were targeted to have an overall 3HV concentration just below 20%, or an in-block concentration of 35−40%. Using these targets, it would be expected that PHBV−PHB−PHBV triblocks would have an overall 3HV concentration of 25−30% if all blocks were the same length. Consequently, values of 3HV % in these fractions of 22% for F3 and 44% for F4 seem reasonable. Further, the *D* statistic calculations indicate block character because they are significantly greater than the value of unity obtained for random copolymers. Finally, the DSC traces are indicative of polymers with two microphases. The glass transitions for both blocks are conserved, as well as the melting temperatures.

Conclusions

One of the major goals of this analysis was to conclusively prove the synthesis of PHA block copolymers within a biological synthesis scheme. Calculating the block copolymer yield was complicated by several factors: the polymer chain heterogeneity, the broad molecular weight distribution as compared to traditional chemical synthesis, and the marginal chemical difference between PHB and PHBV. Without the ability to conclusively prove the structure and composition with standard techniques, combinations of tests that characterize the polymers have been applied. These tests probed the microstructure, composition, and new physical properties that resulted from introducing block copolymer into the polymer structure. Collecting these tests into one analysis suggests that block copolymer formation is likely the linking cause to the compositional and thermal properties observed for the polymer fractions and is also the likely cause for the new properties observed during dynamic and tensile testing.

Commercially viable PHA is often a copolymer of one or more monomers in addition to the 3-hydroxybutyrate units. The main technique to achieve this copolymerization is to feed additional substrates to the bioreactor as described here. Biological synthesis results in a broad chemical compositional distribution (CCD) that may affect the final material properties.[27] If the substrate concentration is not held constant or if nonideal mixing takes place within scaled-up production schemes, the final polymer properties may be difficult to reproduce. These studies show the influence that the copolymerization feeding strategy has on both the CCD and the final PHA material properties.

Because of the biological heterogeneity of the polymerization, the block copolymers synthesized here are statistical blends of several polymer types. Population balance model theory exploring this phenomenon is detailed elsewhere.[17−19] Further, the frequency of the random termination and initiation events will determine the length of time, on average, each individual chain is actively growing. Along with the cofeeding schedule, this turnover frequency will determine the composition along the chain. Consequently, changing the cofeeding schedule will influence the quantity of homopolymer (or random copolymer), diblock copolymer, triblock copolymer, and higher-order block copolymers. These distributions differ significantly from polymers systems synthesized using traditional step-growth or living polymerization techniques.

With new properties achieved from the periodic feeding technique for block copolymers, more characterization work is underway to explain the different rheological and tensile properties observed in the block copolymer samples. Once the relationship between cofeeding time and resulting properties has been determined, the described feedback control technique should prove useful for controlling polymer synthesis with specific and desired properties.

Acknowledgment. The authors thank Qiang Lan for his assistance with dynamical mechanical analysis and Dr. Jack Lewis for assistance with uniaxial testing. This work was supported by the National Science Foundation (BES #0109383) and the National Institute of Health through a training grant in Biotechnology.

References and Notes

(1) Luengo, J. M.; Garcia, B.; Sandoval, A.; Naharro, G.; Olivera, E. R. *Curr. Opin. Microbiol.* **2003**, *6*, 251−260.
(2) Cargill-Dow start-up cultivates biopolymers. *Plast. Eng.* **1998**, *54*, 12−12.
(3) Warwel, S.; Bruse, F.; Demes, C.; Kunz, M.; Rusch gen Klaas, M. *Chemosphere* **2001**, *43*, 39−48.
(4) Lafferty, R. M.; Korsatko, B.; Korsatko, W. In *Biotech*; Rehm, H. J., Ed.; VCH Verlagsgesellschaft: Weinheim, 1988; pp 135−176.
(5) Steinbuchel, A.; Valentin, H. E. *FEMS Microbiol. Lett.* **1995**, *128*, 219−228.
(6) Bates, F. S.; Fredrickson, G. H. *Annu. Rev. Phys. Chem.* **1990**, 525−557.
(7) Bates, F. S. *Science* **1991**, *251*, 898−905.
(8) Abe, H.; Doi, Y.; Kumagai, Y. *Macromolecules* **1994**, *27*, 6012−6017.
(9) Andrade, A. P.; Neuenschwander, P.; Hany, R.; Egli, T.; Witholt, B.; Li, Z. *Macromolecules* **2002**, *35*, 4946−4950.
(10) Ravenelle, F.; Marchessault, R. H. *Biomacromolecules* **2002**, *3*, 1057−1064.
(11) Shuai, X.; Jedlinski, Z.; Luo, Q.; Farhod, N. *Chin. J. Polym. Sci. (Eng. Ed.)* **2000**, *18*, 19−23.

(12) Kumagai, Y.; Doi, Y. *J. Environ. Polym. Degrad.* **1993**, *1*, 81−87.
(13) Vaneechoutte, M.; Kampfer, P.; De Baere, T.; Falsen, E.; Verschraegen, G. *Int. J. Syst. Evol. Microbiol.* **2004**, *54*, 317−327.
(14) Vandamme, P.; Coenye, T. *Int. J. Syst. Evol. Microbiol.* **2004**, *54*, 2285−2289.
(15) Jurasek, L.; Nobes, G. A. R.; Marchessault, R. H. *Macromol. Biosci.* **2001**, *1*, 258.
(16) Marchessault, R. H.; Monasterios, C. J.; Jesudason, J. J.; Ramsay, B.; Saracovan, I.; Ramsay, J.; Saito, T. *Polym. Degrad. Stabil.* **1994**, *45*, 187−196.
(17) Mantzaris, N. V.; Kelley, A. S.; Daoutidis, P.; Srienc, F. *Chem. Eng. Sci.* **2002**, *57*, 4643−4663.
(18) Mantzaris, N. V.; Kelley, A. S.; Srienc, F.; Daoutidis, P. *AIChE J.* **2001**, *47*, 727−743.
(19) Kelley, A. S.; Mantzaris, N. V.; Daoutidis, P.; Srienc, F. *Nanoletters* **2001**, *1*, 481.
(20) Pederson, E. N.; Srienc, F. *Macromol. Biosci.* **2004**, *4*, 243−254.
(21) Doi, Y.; Kunioka, M.; Nakamura, Y.; Soga, K. *Macromolecules* **1987**, *20*, 2988−2991.
(22) Friedrich, C. G.; Friedrich, B.; Bowien, B. *J. Gen. Microbiol.* **1981**, *122*, 69−78.
(23) Pollard, D.; Salmon, P. In *Encyclopedia of Bioprocess Technology: Fermentation, Biocatalysis, and Bioseparation*; Flickinger, M. C., Drew, S. W., Eds.; Wiley: New York, 1999; p 2622.
(24) Riis, V.; Mai, W. *J. Chromatogr.* **1988**, *445*, 229−248.
(25) Yoshie, N.; Menju, H.; Sato, H.; Inoue, Y. *Macromolecules* **1995**, *28*, 6516−6521.
(26) Kamiya, N.; Inoue, Y.; Doi, Y.; Chujo, R.; Yamamoto, Y. *Macromolecules* **1989**, *22*, 1676−1682.
(27) Yoshie, N.; Inoue, Y. *Int. J. Biol. Macromol.* **1999**, *25*, 193−200.
(28) Bluhm, T. L.; Hamer, G. K.; Marchessault, R. H.; Fyfe, C. A.; Veregin, R. P. *Macromolecules* **1986**, *19*, 2871−2876.

BM0510101